Computer Methods and Programs in Biomedicine 150 (2017) 1–8

Contents lists available at ScienceDirect

Computer Methods and Programs in Biomedicine

journal homepage: www.elsevier.com/locate/cmpb

Multi-modal discriminative dictionary learning for Alzheimer's disease and mild cognitive impairment

Qing Li[a], Xia Wu[a,b,*], Lele Xu[a], Kewei Chen[c], Li Yao[a,b], Rui Li[d]

[a] College of Information Science and Technology, Beijing Normal University, Beijing 100875, China
[b] State Key Laboratory of Cognitive Neuroscience and Learning, Beijing Normal University, Beijing 100875, China
[c] Banner Alzheimer's Institute and Banner Good Samaritan PET Center, Phoenix, AZ 850006, USA
[d] Center on Aging Psychology, Key Laboratory of Mental Health, Institute of Psychology, Chinese Academy of Sciences, Beijing 100101, China

ARTICLE INFO

Article history:
Received 27 November 2016
Revised 28 April 2017
Accepted 18 July 2017

Keywords:
Mild cognitive impairment (MCI)
Alzheimer's disease (AD)
Multimodal neuroimaging data
Discriminative dictionary
Brain disorders

ABSTRACT

Background and objective: The differentiation of mild cognitive impairment (MCI), which is the prodromal stage of Alzheimer's disease (AD), from normal control (NC) is important as the recent research emphasis on early pre-clinical stage for possible disease abnormality identification, intervention and even possible prevention.

Methods: The current study puts forward a multi-modal supervised within-class-similarity discriminative dictionary learning algorithm (SCDDL) we introduced previously for distinguishing MCI from NC. The proposed new algorithm was based on weighted combination and named as multi-modality SCDDL (mSCDDL). Structural magnetic resonance imaging (sMRI), fluorodeoxyglucose (FDG) positron emission tomography (PET) and florbetapir PET data of 113 AD patients, 110 MCI patients and 117 NC subjects from the Alzheimer's disease Neuroimaging Initiative database were adopted for classification between MCI and NC, as well as between AD and NC.

Results: Adopting mSCDDL, the classification accuracy achieved 98.5% for AD vs. NC and 82.8% for MCI vs. NC, which were superior to or comparable with the results of some other state-of-the-art approaches as reported in recent multi-modality publications.

Conclusions: The mSCDDL procedure was a promising tool in assisting early diseases diagnosis using neuroimaging data.

1. Introduction

Studies of Alzheimer's disease (AD) and mild cognitive impairment (MCI) have explored varied neuroimaging modalities with promising results. These include structural Magnetic Resonance Imaging (sMRI) [41,52], functional MRI (fMRI) [15,32], Flourodeoxyglucose Positron Emission Tomography (FDG-PET) [23], and amyloid PETs such as Pittsburgh compound B (PiB-PET) [51], florbetapir [27], and flutemetamol [36] PETs. As each single modality offers specific information about MCI or AD, combining the complementary information from different modalities might enhance understanding of AD and MCI [10,29,43,48].

sMRI provides structural information about the cerebrum and has proved that brain regions such as the hippocampus and parahippocampus are most suited for differentiation between MCI and normal controls (NC) [6,11,22,41]. FDG-PET measures glucose metabolism and has indicated that brain regions such as the superior frontal gyrus, and middle cingulate cortex discriminate well between MCI and NC [9,18,23]. Amyloid-PET non-invasively measures the accumulation of amyloid in the brain, and it has suggested that brain regions such as the posterior cingulate and lateral temporal cortices are affected more in MCI than the NC [4,30]. These recent studies demonstrate that each brain-imaging technique can provide specific views about brain function or structure [3]. In other words, biomarkers from these modalities offer different and potentially complementary information about various aspects of a given disease process [2,5,27]. Indeed, multi-modality neuroimaging has been viewed as a research method in neuroscience [31,53].

Numerous studies have reported various ways of combining multi-modality data for efficient classification [8,10,16,33,34,42,50] and better differentiation of patients with AD or MCI from cognitively healthy individuals. For example, a weighted multiple kernel learning (MKL) model has been applied

* Corresponding author at: College of Information Science and Technology, Beijing Normal University, No. 19 Xin Jie Kou Wai Da Jie, Beijing 100875, China.
E-mail addresses: liqing_lq@mail.bnu.edu.cn (Q. Li), wuxia@bnu.edu.cn (X. Wu), xulelebnu@gmail.com (L. Xu), Kewei.Chen@bannerhealth.com (K. Chen), yaoli@bnu.edu.cn (L. Yao), lir@psych.ac.cn (R. Li).

http://dx.doi.org/10.1016/j.cmpb.2017.07.003
0169-2607/

Table 1
Demographic information of the subjects, *p*-value was obtained using one-way ANOVA to the AD, MCI, and NC groups.

	AD (n= 113; 62 M/51F)			MCI (n= 110; 59 M/51F)			NC (n= 117; 62 M/55F)		
	Mean	SD	Range	Mean	SD	Range	Mean	SD	Range
Age	75.6	7.6	58–90	75.2	7.8	59–91	75.4	7.0	56–94
MMSE	22.4	2.2	20–26	27.4	1.9	24–30	28.9	1.3	26–30
CDR	0.8	0.2	0.5–1	0.5	0.0	0.5–0.5	0.0	0.0	0.0–0.0
EDU	16.10	3.00	9–20	16.57	2.76	9–20	16.44	2.41	12–20
APOE4(%)	50.00	–	–	52.73	–	–	24.49	–	–

Note: AD, Alzheimer's disease; MCI, mild cognitive impairment; NC, normal control; M, male; F, female; MMSE, Mini-Mental State Examination; CDR, Clinical Dementia Rating; EDU, year of education.

to combine cerebrospinal fluid (CSF), MRI, and PET to produce more powerful classifiers of MCI [16]. A linear weighted random forest (RF) model could combine different modalities and discriminate AD or MCI from NC effectively [8]. To utilize both the basic simple features and complex latent representation, multi-kernel SVM learning has been applied [33,34,42]. These studies demonstrate that the weighted combination approach is a simple yet effective way to integrate information from multi-modality data.

Recently, weighted multi-modality sparse representation-based classification (mSRC) has been introduced among neuroimaging communities and has demonstrated its feasibility and effectiveness in discriminating AD or MCI from NC by using data from sMRI, FDG-PET, and florbetapir-PET [44]. However, there are some weaknesses in mSRC as it is based on the SRC method that uses all the training data as a dictionary. When faced with large training sets, the sparse representation of a dictionary might be computationally time-consuming [13]. In addition, when training samples are not very representative, the classification accuracy would be affected by the dictionary [46].

A recently introduced method in pattern recognition and machine learning by Xu et al. considered supervised within-class-similarity discriminative dictionary learning (SCDDL) a robust and efficient method for facial recognition [45]. To improve the accuracy of facial recognition, SCDDL incorporated the term "within-class-similarity" for representation coefficients into the objective function of dictionary-learning. This is a combination of Fisher Discrimination Dictionary Learning (FDDL) [47] and Discriminative K-SVD (D-KSVD) [49] or Label Consistent K-SVD (LC-KSVD) [12]. wm-SRC in combination with a linear classification error term has been introduced. This aims to derive a more compact dictionary as compared with SRC [45]. Although its first application was in facial-recognition (2-dimensional data), we believe that SCDDL has potential promise in the field of neuroimaging data, especially in multi-modal data for differentiation of AD or MCI from NC.

The contributions of this study are as follows. First, the SCDDL method was extended from single to multiple modalities based on weighted combination (mSCDDL), and was examined with regard to its robustness and accuracy of differentiating NC from MCI or AD. For this study, the multi-modal data used in SCDDL and mSCDDL were sMRI, FDG-PET, and florbetapir-PET. Second, the mSCDDL method was compared with other state-of-the-art multi-modality classification algorithms for performance in differentiating NC from MCI or AD.

2. System and methods

2.1. Participants

The datasets used in this study were downloaded from the Alzheimer's Disease Neuroimaging Initiative (ADNI) (http://www.loni.ucla.edu/ADNI/). A $60 million 5-year project, the ADNI was launched in 2003 by the National Institute on Aging (NIA), National Institute of Biomedical Imaging and Bioengineering (NIBIB), Food and Drug Administration (FDA), private pharmaceutical companies, and non-profit organizations.

According to ADNI protocols, the severity of cognitive impairment was assessed using Mini-Mental State Examination (MMSE) [7] and Clinical Dementia rating (CDR) scores [21]. Individuals assigned to the probable AD group met the National Institute of Neurological and Communicative Disorders Association (NINCDS/ADRDA) criteria [20]. More information is available at http://adni.loni.usc.edu/about/.

All the data including sMRI, FDG-PET and florbetapir PET were downloaded from 2014/03/23 to 2014/05/12, in ADNI 1, ADNI GO and ADNI 2. For each subject, the data-acquisition interval of the three modalities was within four months. And if some subjects had several times detection, we just used the first one. In total, 113 patients with AD (51 female and 62 male patients; mean age, 75.6 years; mean MMSE, 22.4 [range, 20–26]; CDR, 0.5 or 1), 110 patients with MCI (51 female and 59 male patients; mean age, 75.2 years; mean MMSE, 27.4 [range, 24–30]; CDR, 0.5), and 117 NC (55 female and 62 male patients; mean age, 75.4 years; mean MMSE, 28.9 [range, 26–30]; CDR, 0) were included in this study. The age of all the subjects ranged from 55 to 99 years. The AD group did not significantly differ from the NC group with respect to age ($p = 0.945$) and the duration of education ($p = 0.690$); however, the AD group had significantly lower MMSE scores ($p = 1.24 \times 10^{-90}$) and more presence of APOE E4 alleles ($p = 0.014$) than the NC group. The AD group did not significantly differ from the MCI group with respect to age ($p = 0.760$), the duration of education ($p = 0.624$), and l presence of APOE E4 alleles ($p = 0.765$); however, the AD group had significantly lower MMSE scores ($p = 1.61 \times 10^{-40}$) than the MCI group. The MCI group did not significantly differ from the NC group with respect to age ($p = 0.698$) and the duration of education ($p = 0.808$); however, the MCI group had significantly lower MMSE scores ($p = 4.69 \times 10^{-31}$) and more presence of APOE E4 alleles ($p = 7.34 \times 10^{-04}$). The demographic information of the subjects is shown in Table 1.

2.2. Data processing

The spatial preprocessing of the structural MRI data was performed using the VBM8 (Voxel-Based Morphometry 8) Toolbox (http://dbm.neuro.uni-jena.de/vbm8) in SPM8 (Scanning Probe Microscope 8) (http://www.fli.ion.ucl.ac.uk/spm). There were two main steps: segmentation and normalization. Based on adaptive maximum posterior and partial volume estimation, every structural image was segmented into rigid-body-aligned grey matter, white matter, and CSF for each subject [25,37]. To improve the segmentation, spatially adaptive non-local, which meant denoising filter [17] and classical Markov Random Field approach were applied. The exponential Lie algebra (DARTEL) protocol [1] in which template creation and image registration were performed iteratively, was used to normalize the grey-matter images by using a

diffeomorphic anatomical registration. A single constant-velocity field was used to generate diffeomorphic and invertible deformations in DARTEL. In each of the iterations, the individual brain-tissue maps registered a newly created template, and the grey-matter tissue maps were normalized in Montreal Neurological Institute (MNI) space. After this, Jacobian determinants multiplied the registered grey-matter maps with non-linear warping in order to exclude individual differences in total intracranial volume.

Using a rigid body transformation, all FDG-PET and florbetapir-PET images were co-registered with each individual's sMRI and subsequently warped to the cohort-specific DARTEL template. Thereafter, the standard uptake value ratio (SUVr) image was calculated for each FDG-PET image that was defined relative to the whole brain as a reference mask [14,19]. For florbetapir-PET images, it was defined relative to the cerebellum as the reference mask, because the cerebellum has been reported to be a region free of fibrillar amyloid plaques in AD brains [4,26].

2.3. Feature extraction

Ninety regions of interest (ROIs) (45 for each hemisphere; Table S2) were first defined by Automated Anatomical Labeling (AAL) [38]. Further, for each subject, the mean volume of gray matter, SUVr values of FDG, and florbetapir-PET from each ROI were computed by averaging the corresponding value of all the voxels within that ROI. This was performed as a feature of MRI, FDG-PET, and florbetapir-PET, respectively, for further analysis.

2.4. Classification on MCI and AD

The single-modality results based on SCDDL (SCDDL-sMRI, SCDDL-FDG-PET, and SCDDL-florbetapir-PET) and multi-modality results from several other state-of-the-art multi-modality methods (MKL, JRC, and mSRC) were compared with results of multi-modality SCDDL (mSCDDL). The first method MKL was based on a support vector machine (SVM) that combined kernels from different modalities with corresponding kernel weights that were optimized by the grid search approach [8,16,50]. The second method JRC (Joint Regression and Classification) concatenated multi modalities into one vector first, and then adopted high-level information inherent such as sample-sample and variable-variable relations (variable indicated clinical scores and class label, in this study, variables were the clinical score of MMSE and the class label) for joint feature selection [54,55]. The third method mSRC combined multi-modality data into a large vector based on direct-feature concatenation that was very simple and effective [44]. Our mSCDDL method also concatenated multi-modalities directly similar to the mSRC method. All these multi-modality methods were applied to discriminate AD and MCI from NC based on sMRI, FDG-PET, and florbetapir-PET data.

To evaluate the methods, their accuracy, sensitivity, and specificity were calculated. Accuracy is the ratio of samples correctly classified among the test samples. Sensitivity is the ratio of positive classes that were correctly identified, and specificity is the ratio of negative classes that were accurately classified. Further, the areas under the ROC curve (AUC) based on single modality SCDDL and some other multi-modality methods were compared with those from mSCDDL. And the two-sample *t*-test was performed on accuracy, sensitivity, specificity and AUC respectively.

In this study, subjects from each group (AD, MCI, and NC) were divided into training and test sets. Sixty subjects (samples) were selected randomly as the training set, and the test set consisted of the rest of the subjects (samples). The process of division was then repeated 10 times. The results of means and standard deviations based on the data sets are reported in this paper.

3. Algorithm

All the features extracted from three modalities of data (sMRI, FDG-PET, and florbetapir-PET) were included for the differentiation of AD and MCI from NC. The supervised within-class-SCDDL was presented for the first time in this section and was applied to neuroimaging data to classify MCI and AD from NC. Further, the extended multi-modality framework based on SCDDL, termed as multi-modality SCDDL (mSCDDL), was applied to the combined multi-modality data to differentiate NC from MCI and AD because the multi-modality method could provide more information from different modalities and enhance understanding of MCI [29,48].

3.1. Supervised within-class-similar discriminative dictionary learning (SCDDL)

SCDDL was postulated by Xu et al. [44]; its classification model can be simply described as follows:

If the d-dimensional n training samples from k classes are denoted by $A=[A_1,..., A_l..., A_k] \in \Re^{d\times n}$, in each sub-matrix, each column represents data from one subject, and each row represents features from one ROI. The discriminant dictionary with m atoms that needs to be learned, is represented by $D \in \Re^{d\times m}$ ($m \le n$). This representation coefficient of A on D is represented by X that can be denoted as $X=[X_1,\ldots,X_i,\ldots,X_k] \in \Re^{m\times n}$. Thus, the SCDDL model can be written as follows:

$$\langle D,W,X\rangle = \arg\min_{D,W,X} \|A-DX\|_F^2+\alpha\|H-WX\|_F^2 +\beta\|W\|_F^2+\lambda_1\|X\|_1+\lambda_2\sum_{i=1}^{k}\left(\|X_i-M_i\|_F^2+\eta\|X_i\|_F^2\right), \quad (2)$$
$$s.t.\left\|d_j\right\|_2^2=1, for\ all\ j=1,...,m$$

The reconstructed error term of the training samples A on the newly learned dictionary D is denoted by $\|A-DX\|_F^2$, the linear classification error term is represented by $\alpha\|H-WX\|_F^2+\beta\|W\|_F^2$, and the within-class-similar term is represented by $\sum_{i-1}^{k}(\|X_i-M_i\|_F^2+\eta\|X_i\|_F^2)$. The parameter of the classifier is denoted by $W \in \Re^{k\times m}$; each training sample corresponds to each column of $H \in \Re^{k\times n}$ that is a vector like [0, 0, ..., 1..., 0, 0] $\in \Re^k$. In this equation, the corresponding class of the training sample is located by 1; the mean vector of representation coefficients X_i is represented by each column of M_i that corresponds to class i; each row of matrix D is represented by d_j. To further stabilize the solution of Eq. (2), according to the elastic-net theory, the term $\|X_i\|_F^2$ is combined with the term $\|X\|_1$ [56]. To simplify, η is set as $\eta=1$ [47]. Then, Eq. (2) can be written as:

$$\langle D,W,X\rangle = \arg\min_{D,W,X} \|A-DX\|_F^2+\alpha\|H-WX\|_F^2+\beta\|W\|_F^2 +\lambda_1\|X\|_1+\lambda_2\sum_{i=1}^{k}\left(\|X_i-M_i\|_F^2+\|X_i\|_F^2\right), \quad (3)$$
$$s.t.\left\|d_j\right\|_2^2=1,\ \ for\ all\ j=1,...,m$$

In SCDDL, to make the coding coefficients similar within one class, the within-class-similar term was added. To enable the optimal classifier corresponding to the dictionary, the linear classification error term was added. Therefore, the discriminatory power of the dictionary for classification can be enhanced through this approach.

3.2. Multi-modality supervised within-class-similar discriminative dictionary learning (mSCDDL)

The above SCDDL model was defined for the classification of single-modality data. Previous researchers have revealed that

combination of multi-modality features is helpful in classification [29,48]. The weighted combination manner is a simple but efficient way for combining different modalities [8,10,44]. Therefore, the SCDDL model was expanded to multi-modality SCDDL (mSCDDL) through the weighted combination method.

Suppose d-dimensional n training samples from k classes are denoted by $A=[A_1,...,A_l...,A_k]\in\Re^{d\times n}$. If P modalities are contained in each sample, then the training sample A^p could be denoted by $A^p=[A_1^p,...,A_l^p,...,A_K^p](l=1,2,...,K)$ that comes from the feature $p(p=1,2,...,P)$. Then the coefficient of the corresponding dictionary $D^p\in\Re^{d\times q}(q\le n)$ for the training sample A^p is $X^p=[X_1^p,...,X_l^p,...,X_K^p]\in\Re^{q\times n}$ in which q dictionary atoms for learning are included. Therefore, mSCDDL could be calculated as follows:

$$\begin{aligned}&\left\langle D^1,...,D^P,W^1,...,W^P,X^1,...,X^P\right\rangle\\&=\arg\min_{\substack{D^1,...,D^P,\\W^1,...,W^P,\\X^1,...,X^P}}\sum_{p=1}^{P}\|A^p-D^pX^p\|_F^2+\alpha^p\|H^p-W^pX^p\|_F^2\\&+\lambda_1^p\|X^p\|_1+\lambda_2^p\sum_{i=1}^{K}\left(\left\|X_i^p-M_i^p\right\|_F^2+\left\|X_i^p\right\|_F^2\right)\end{aligned},\quad(4)$$

The dictionary D^p and classifier W^p of each feature p could be obtained according to the SCDDL algorithm and applied for classifying the test data from Eq. (4). More specifically, the coefficients of $D=[D^1,...,D^p,...,D^P]$ for a given sample $y=[y^1,...,y^p,...,y^P]$ could be calculated using Eq. (5):

$$\left\langle x^1,...,x^p...,x^P\right\rangle=\arg\min_{x^1,...,x^P}\sum_{p=1}^{P}\|y^p-D^px^p\|_2+\lambda\|x^p\|_1,\quad(5)$$

The regularization constant of this is denoted by λ, and $x^p(p=1,...,P)$ is a vector that is a coefficient containing the discriminative information for classification.

To obtain the final label for the test sample y, the weighted combination method was used as follows:

$$\begin{cases}label(y)=\arg\max_l\left\{\sum_{p=1}^{P}\omega_pW^px^p\right\}_l,l=1,2,...,K\\\sum_{p=1}^{P}\omega_p=1\\\omega_p\ge0,p=1,...,P\end{cases},\quad(6)$$

The weight coefficients in this equation are denoted by $\omega_p(p=1,...,P)$ to balance the contribution of each feature for classification. To optimize the ω_p, either a grid search approach through 10-fold cross-validation on the training samples was used [8,44,45] or simply set as 1/P (this assumes that the contribution of each feature is equal for classification).

After the optimal value of ω has been determined, the class label for the test sample could be assigned according to Eqs. (4)–(6). Further, the performance of mSCDDL could be evaluated by calculating the accuracy, sensitivity, and specificity of the test samples.

4. Results

4.1. Comparison with single-modality SCDDL

To compare the results more easily, the dictionary size was set as 20 atoms for both SCDDL and mSCDDL. The performances of single-modality SCDDL (SCDDL-sMRI, SCDDL-FDG-PET, and SCDDL- florbetapir-PET) and multi-modality mSCDDL (sMRI + FDG-PET + florbetapir-PET) were evaluated. The multi-modality mSCDDL achieved higher accuracy in classifying MCI or AD from NC than all the single-modality methods as shown in Fig. 1 and Table 2.

For classifying MCI from NC, the mSCDDL achieved an accuracy of 77.66% (with sensitivity of 75.00% and specificity of 80.70%). This result was numerically better than any of single-modality methods (the best classification accuracy was 72.50%, $p=0.143$ when using SCDDL-FDG-PET). Further, the AUC was 0.828 for the multi-modality method that was greater than that of the single-modality methods (AUC = 0.787 for SCDDL-sMRI, and $p=0.405$ for compared with multi-modality method; AUC = 0.762 for SCDDL-FDG-PET, and $p=0.098$ compared with multi-modality method; AUC = 0.742 for SCDDL-florbetapir-PET, and $p=0.074$ compared with multi-modality method). The comparison of the ROC curves for classification of MCI and NC are shown in Fig. 1(a). The ROC curve of mSCDDL was closer to the top-left corner than that of SCDDL-sMRI and SCDDL-florbetapir-PET and much closer to the top-left corner than SCDDL-FDG-PET. This implies that the mSCDDL method was more outperformed than SCDDL-sMRI and SCDDL-florbetapir-PET, and slightly exceled than the SCDDL-FDG-PET.

For discriminating AD from NC, the mSCDDL achieved an accuracy of 97.36% (with 99.25% sensitivity and 95.61% specificity) that was a little better statistically and numerically superior to the best accuracy of 91.18%, $p=0.142$ with single-modality methods (using SCDDL-FDG-PET). Further, the area under the ROC curve (AUC) was 0.985 with mSCDDL and this method was greater than the single-modality methods (AUC = 0.939 for SCDDL-sMRI, $p=0.046$ for compared with multi-modality method; AUC = 0.970 for SCDDL-FDG-PET, $p=0.270$ for compared with multi-modality method; and AUC = 0.937 for SCDDL-florbetapir-PET, $p=0.049$ for compared with multi-modality method). The comparison of the ROC curves for classification of AD and NC is shown in Fig. 1(b). The ROC curve of mSCDDL was closer to the top-left corner than that of SCDDL-FDG-PET and SCDDL-florbetapir-PET and much closer to the top-left corner than that of the SCDDL-sMRI. This means that the mSCDDL method was more outperformed than SCDDL-FDG-PET and SCDDL-florbetapir-PET and slightly exceled than SCDDL-sMRI.

Particularly, the combined weight parameters ω in mSCDDL (that was optimized by the grid search approach) for sMRI, FDG-PET, and florbetapir-PET were 0.4, 0.4, and 0.2, respectively, for differentiating AD from NC and 0.2, 0.7, and 0.1, respectively, for differentiating MCI from NC.

4.2. Comparison with several other multi-modality methods

4.2.1. Test time

mSCDDL was further compared with several other multi-modality methods (MKL, JRC, mSRC) for test time. The test time is the computational time corresponding algorithms need for classification of per test samples. The dictionary size was also set as 20 atoms for mSCDDL.

The test times for different methods are shown in Fig. 2. From the figure, it could be seen that the mSCDDL method consumed much less time for classification than JRC ($p=0.011$ for MCI and NC; $p=0.011$ for AD and NC) and mSRC ($p=0.020$ for MCI and NC; $p=0.011$ for AD and NC). And though the test time of MKL was shorter than mSCDDL method ($p=0.054$ for MCI and NC; $p=0.030$ for AD and NC), the under 3s gap made no difference practically in clinical diagnosis on case by case basis.

4.2.2. Classification accuracy

The recognition rate of the mSCDDL method was compared with those of several other multi-modality methods (MKL, JRC, and mSRC) for differentiating MCI or AD with NC.

For the differentiation of MCI and NC, mSCDDL achieved an accuracy of 77.66%, which was equally in statistically, but superior to that of the MKL (74.77%, $p=0.202$ for comparing with mSCDDL), JRC (73.83%, $p=0.174$ for comparing with mSCDDL), and mSRC (75.70%, $p=0.371$ for comparing with mSCDDL) methods in numerically as shown in Table 3. The comparison of the ROC curves

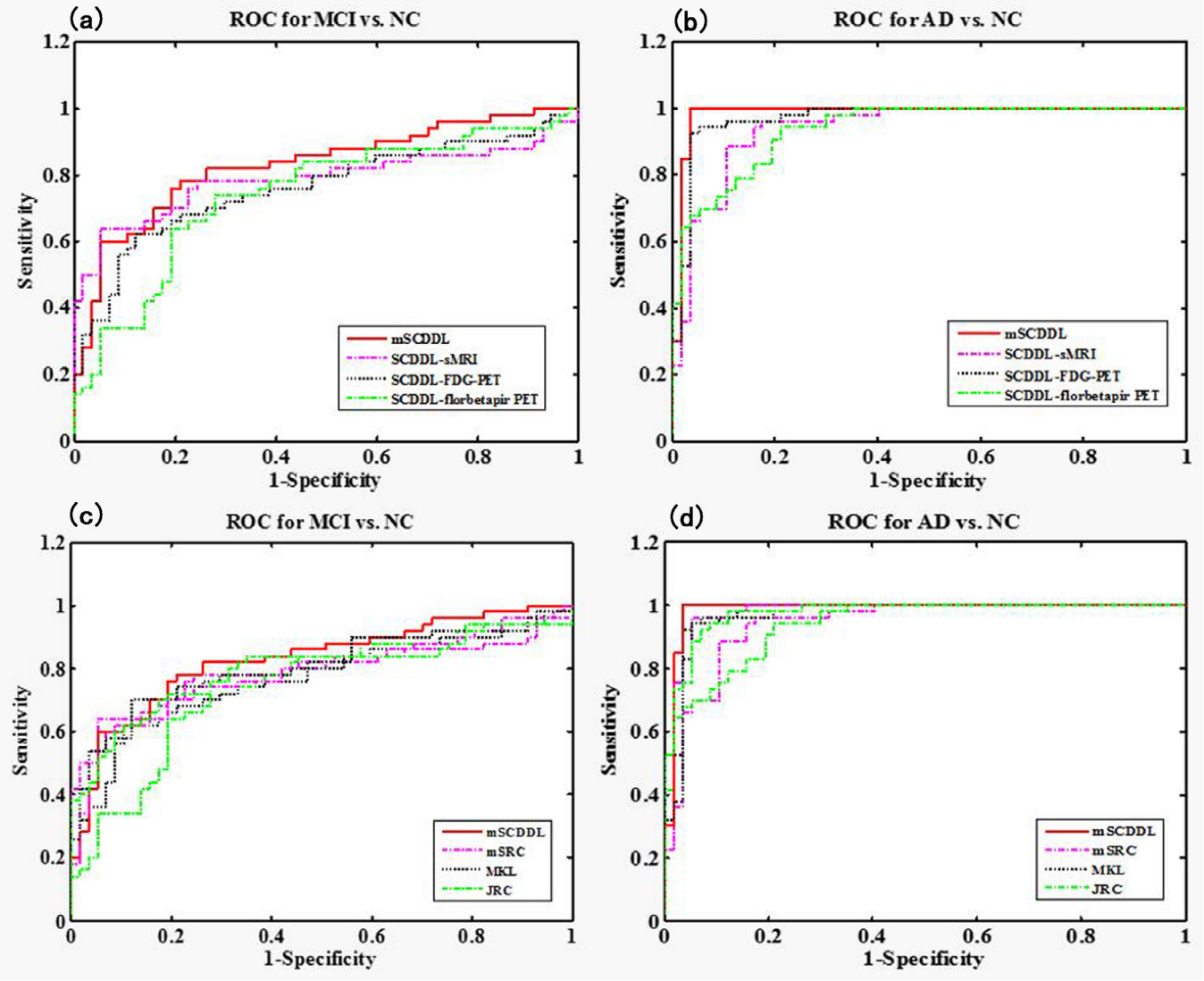

Fig. 1. ROC curves of four different classification methods, including single-modality methods based on SCDDL (SCDDL-sMRI, SCDDL-FDG-PET and SCDDL-florbetapir PET) and mSCDDL for (a) MCI classification, (b) AD classification; ROC curves of four different classification methods, including mSCDDL, mSRC, MKL, and JRC for (c) MCI classification, (d) AD classification.

Table 2
Comparison of the performance of single-modality (SCDDL-sMRI, SCDDL-FDG-PET, and SCDDL-florbetapir-PET) and multi-modality methods based on mSCDDL.

Methods	MCI vs. NC				AD vs. NC			
	ACC (%)	SE (%)	SP (%)	AUC (%)	ACC (%)	SE (%)	SP (%)	AUC (%)
SCDDL-sMRI	71.96	69.80	72.11	78.70	88.27	94.53	82.46	93.90
SCDDL-FDG-PET	72.50	62.20	81.23	76.20	91.18	86.42	95.61	97.00
SCDDL-florbetapir-PET	70.09	66.00	73.68	74.20	85.64	85.51	85.61	93.70
mSCDDL	77.66	75.00	80.70	82.80	97.36	99.25	95.61	98.50

Note: AD, Alzheimer's disease; MCI, mild cognitive impairment; NC, normal control; ACC, classification accuracy; SE, classification sensitivity; SP, classification specificity; AUC, the area under the ROC curve. All the results had 10 folder cross-validations.

Table 3
Comparison of the performances of different multi-modality methods (MKL, JRC, mSRC, and mSCDDL).

Methods	MCI vs. NC				AD vs. NC			
	ACC (%)	SE (%)	SP (%)	AUC (%)	ACC (%)	SE (%)	SP (%)	AUC (%)
MKL	74.77	74.00	75.44	80.40	93.64	96.23	91.23	96.30
JRC	73.83	72.00	75.44	79.30	94.55	98.11	91.23	97.10
mSRC	75.70	66.00	84.21	78.50	94.55	96.23	92.98	97.80
mSCDDL	77.66	75.00	80.70	82.80	97.36	99.25	95.61	98.50

Note: AD, Alzheimer's disease; MCI, mild cognitive impairment; NC, normal control; ACC, classification accuracy; SE, classification sensitivity; SP, classification specificity; AUC, the area under the ROC curve.

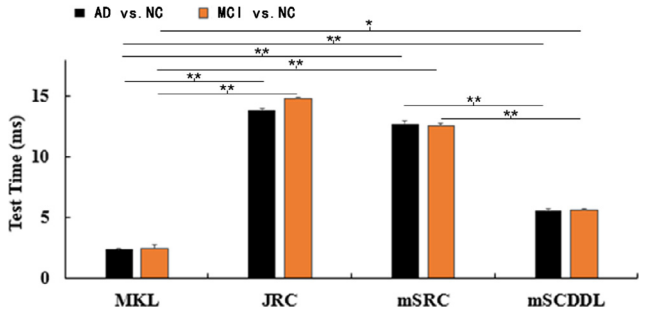

Fig. 2. Comparison of test times for different multi-modality methods (MKL, JRC, mSRC, and mSCDDL) (*indicates $0.05 \le p < 0.1$; **indicates $0.01 \le p < 0.05$).

for differentiation of MCI and NC is shown in Fig. 1(c). The ROC curve of mSCDDL was closer to the top-left corner than that of mSRC and JRC, and was comparable with that of MKL. This implied that mSCDDL was more stable and outperformed than mSRC and JRC, and comparable with MKL.

For the differentiation of AD and NC, mSCDDL achieved an accuracy of 97.36% for discriminating AD from NC that was equally in statistically, but superior to MKL (93.64%, $p = 0.157$ compared with mSCDDL), JRC (94.55%, $p = 0.236$ compared with mSCDDL), and mSRC (94.55%, $p = 0.255$ compared with mSCDDL) methods in numerically. This indicated that the mSCDDL was an efficient method for the purpose. The comparison of the ROC curves for classification of AD and NC is shown in Fig. 1(d). The ROC curve of mSCDDL was closer to the top-left corner than that of mSRC, MKL, and JRC. This implied that mSCDDL was more outstanding than mSRC, MKL, and JRC for differentiation between AD and NC.

The areas under the ROC curves for differentiation of MCI or AD based on the four different methods are compared in Table 3, in which the mSCDDL method (AUC = 0.828 for AD detection, and AUC = 0.985 for AD detection) performed much greater than the other three multi-modality methods (AUC = 0.804 for MKL, $p = 0.534$ for compared with mSCDDL; AUC = 0.793 for JRC, $p = 0.331$ for compared with mSCDDL; and AUC = 0.785 for mSRC, $p = 0.223$ for compared with mSCDDL in AD detection; AUC = 0.963 for MKL, $p = 0.130$ for compared with mSCDDL; AUC = 0.971 for JRC, $p = 0.359$ for compared with mSCDDL; and AUC = 0.978 for mSRC, $p = 0.655$ for compared with mSCDDL in AD detection).

5. Discussion

In this study, a multi-modality classification method, mSCDDL was extended from single modality and compared with other state-of-the-art multi-modality methods (MKL, JRC, and mSRC) to identify AD and MCI. Three modalities, namely sMRI, FDG-PET, and florbetapir-PET, were used. The results revealed the effectiveness of mSCDDL for differentiation between AD and MCI (97.36% for AD and 77.66% for MCI). And the mSCDDL method was compared with other state-of-the-art multi-modality classification algorithms for performance in differentiating NC from MCI or AD.

5.1. Comparison with signal-modality SCDDL

The mSCDDL achieved superior classification accuracy than the methods based on single-modality SCDDL (SCDDL-sMRI, SCDDL-FDG-PET, and SCDDL-florbetapir-PET), as seen in the results. Further, for both MCI and AD classification, the AUC of mSCDDL was greater than that of single-modality methods, either statistically or numerically. Our results were also consistent with those of other studies. Platt and Walhovd reported that different modalities could supply complementary information [24,39,40]. Other studies reported that combining multiple modalities could obtain more excellent classification accuracy (Gary et al., 2013; [43,44,50]).

Notably, on differentiating between MCI and NC, the classification specificity based on SCDDL-FDG-PET was 81.23%, which was slightly higher than that based on mSCDDL (80.70%), whereas the classification sensitivity based on SCDDL-FDG-PET (62.20%), which was not acceptable in clinical, was much lower than that of mSCDDL (75.00%). Lower sensitivity with only marginally higher specificity (which could be due to random noise) would result in underdiagnosis. The mSCDDL method had higher sensitivity and outstanding specificity that was comparable with that of SCDDL-FDG-PET, and much higher than that of the other methods. Therefore, the results suggest the feasibility of using mSCDDL for neuroimaging classification tasks.

5.2. Comparison with several other multi-modality methods

The classification accuracy results of MCI or AD indicated that mSCDDL (97.36% for AD classification, 77.66% for MCI classification) was more preferable than several other multi-modality classification methods such as MKL, JRC, and mSRC [44,50,54] in Table 3. In general, the AUC of mSCDDL was either significantly or at least numerically greater than that of the other methods.

Additionally, the computation time of mSCDDL was lesser than that of JRC and mSRC, and was comparable with that of MKL. Therefore, mSCDDL, an ensemble-learning weighted-combination method, was a simple but efficient way for multi-feature combination.

5.3. Comparison with several published works on biomarkers

The classification accuracy rate and AUC of the mSCDDL method with sMRI, FDG-PET and florbetapir-PET were compared with those of several other published works with cerebrospinal fluid (CSF), genetic, etc. in Table S1.

CSF is a commonly used fluid biomarker which has been used to predict MCI or AD from NC in several studies. For classifying MCI and NC, the accuracy were 63.10% [8], 68.30% [34] and 71.40% [50], and for classifying AD and NC, the accuracy were 76.50% [8], 83.10% [34] and 82.10% [50] separately. People have also attempted to use APOE information for AD/MCI classification with NC. The corresponding classifying accuracy was 73.80% in predicting MCI from NC and 72.60% in predicting AD from NC [8].

Beside these studies with uni-biomarker, there were several taking multimodal approaches. Hinrichs et al. have used MRI, PET, CSF, APOE and cognitive to predict AD from NC, and got the promising accuracy of 92.40% [10]. And, Zhang et al. have taken MRI, PET and CSF to do the same study and got equally impressive 93.20% [50].

In general, the classification accuracy of all these studies were compatible to our results (77.66% for MCI NC classification, and 97.36% for AD NC classification). Though not possible for use to statistically compare ours to these published ones, numerically, the accuracy of our method was higher or not worse than them.

5.4. Comparison of classifying APOE carriers and APOE non-carriers

To compare the performance of APOE carriers and APOE non-carriers, the classification accuracy of single-modality SCDDL (SCDDL-sMRI, SCDDL-FDG-PET, and SCDDL-florbetapir-PET) and multi-modality mSCDDL (sMRI + FDG-PET + florbetapir-PET) were evaluated. The multi-modality mSCDDL achieved higher accuracy in classifying APOE carriers from APOE non-carriers than all the single-modality methods as shown in Table S2.

The mSCDDL achieved an accuracy of 63.16%, which was more accurate than the single-modality methods (accuracy of 57.05%

for SCDDL-sMRI, $p = 0.165$ compared with mSCDDL; accuracy of 58.74% for SCDDL-FDG-PET, $p = 0.016$ compared with mSCDDL; accuracy of 61.47% for SCDDL-florbetapir-PET, $p = 0.173$ compared with mSCDDL).

Though, the mSCDDL method didn't perform better statistically than SCDDL-florbetapir-PET, the numerably improvement was a sensational promotion, which also meant the mSCDDL method was a useful method not only on classifying AD/MCI from NC, but also on classifying APOE carriers from APOE non-carriers.

6. Limitations

This study had several limitations. First, many other data sources are useful for AD or MCI classification in addition to sMRI, FDG-PET, and florbetapir-PET, such as cerebrospinal fluid (CSF) [28,35,50]. Second, only the weighted combination method was used in this study for the multi-modality analysis. Additional studies could attempt to expand SCDDL to multi-modal ones in the framework of multi-kernel learning. Third, this study did not include the cognition information in the classification method focusing on the imaging modalities only. Future studies would examine cognition together with neuroimaging data and possibly others (such as genomics), which we hypothesize will be with further improvements.

7. Conclusions

This study proposed a multi-modality-supervised within-class-similar discriminative dictionary learning classifier called "mSCDDL" to combine the multi-modality features (sMRI, FDG-PET, and florbetapir-PET) for differentiating AD and MCI from NC. The results suggest that the mSCDDL procedure is a promising tool for classification especially in helping to diagnose diseases using neuroimaging data.

Funding information

This work was supported by the Funds for International Cooperation and Exchange of the National Natural Science Foundation of China [grant number 61210001], the General Program of National Natural Science Foundation of China [grant number 61571047], and the Fundamental Research Funds for the Central Universities [grant number 2017EYT36].

Acknowledgements

The data set used in preparation of this paper was obtained from the Alzheimer's Disease Neuroimaging Initiative (ADNI) database (adni.loni.ucla.edu). As such, the investigators within the ADNI contributed to the design and implementation of ADNI and/or provided data but did not participate in the analysis or writing of this report. A complete listing of ADNI investigators can be found at: http://adni.loni.ucla.edu/wcontent/uploads/how_to_apply/ADNI_Acknowledgement_ist.pdf.

Declaration of interest

(1) There are no actual or potential conflicts of interest.

(2) There is no author's institution has contracts relating to this research through which it or any other organization may stand to gain financially now or in the future.

(3) All of the authors could be seen as involving a financial interest in this work.

Submission declaration and verification

The work described has not been published previously, and will not be submitted elsewhere while under consideration at Pattern Recognition.

All authors have reviewed the contents of the manuscript being submitted, approve of its contents and validate the accuracy of the data.

Supplementary materials

Supplementary material associated with this article can be found, in the online version, at doi:10.1016/j.cmpb.2017.07.003.

References

[1] J. Ashburner, A fast diffeomorphic image registration algorithm, Neuroimage 38 (1) (2007) 95–113.
[2] C.M. Bauer, Multimodal Analysis in Normal Aging, MildCognitive Impairment, and Alzheimer's Disease: Group Differentiation, Baseline Cognition and Prediction of Future Cognitive Decline, Boston University, 2013.
[3] V.D. Calhoun, et al., A method for multitask fMRI data fusion applied to schizophrenia, Human Brain Mapp. 27 (2006) 598–610.
[4] V. Camus, et al., Using PET with 18F-AV-45 (florbetapir) to quantify brain amyloid load in a clinical environment, Eur. J. Nucl. Med. Mole. Imag. 39 (4) (2012) 621–631.
[5] K. Chen, et al., Correlations between FDG PET glucose uptake-MRI graymatter volume scores and apolipoprotein E (4 gene dose incognitively normal adults: a cross-validation study usingvoxel-based multi-modal partial least squares, Neuroimage 60 (4) (2012) 2316–2322.
[6] Y. Fan, et al., Spatialpatterns of brain atrophy in MCI patients, identified viahigh-dimensional pattern classification, predict subsequentcognitive decline, Neuroimage 39 (4) (2008) 1731–1743.
[7] M.F. Folstein, et al., "Mini-mental state": a practical method for grading the cognitive state of patients for the clinician, J. Psychiatr. Res. 12 (1975) 189–198.
[8] K.R. Gray, et al., Random forest-based similarity measures for multi-modal classification of Alzheimer's disease, Neuroimage 65 (2012) 167–175.
[9] S.D. Gretel, et al., Glucose metabolism during resting state reveals abnormal brain networks organization in the Alzheimer's disease and mild cognitive impairment, PLoS One 8 (7) (2013) e68860.
[10] V. Hinrichs, et al., Predictive markersfor AD in a multi-modality framework: an analysis of MCI progression in the ADNI population, Neuroimage 55 (2) (2011) 574–589.
[11] C.R. Jack, et al., Prediction of AD with MRI-based hippocampal volume inmild cognitive impairment, Neurology 52 (7) (1999) 1397.
[12] Z. Jiang, et al., Label consistent K-SVD: learning a discriminative dictionary for recognition, IEEE Trans. Pattern Anal. Mach. Intel. 35 (2013) 2651–2664.
[13] S.M. Landau, et al., Comparing predictors of conversion and decline inmild cognitive impairment, Neurology 75 (3) (2010) 230–238.
[14] J.B.S. Langbaum, K Chen, W Lee, et al., Categorical and correlational analyses of baseline fluorodeoxyglucose positron emission tomography images from the Alzheimer's disease neuroimaging initiative (ADNI), Neuroimage 45 (4) (2009) 1107–1116.
[15] D. Lenzi, et al., Single domain amnestic MCI: a multiple cognitive domains fMRI investigation, Neurobiol. Ag. 32 (9) (2011) 1542–1557.
[16] F. Liu, et al., Multiple Kernel learning in the primal for multimodal Alzheimer's disease classification, IEEE J. Biomed. Health Inform. 18 (3) (2014) 984–990.
[17] J.V. Manjón, et al., Adaptive non-local means denoising of MR images with spatially varying noise levels, J. Magn. Reson. Imag. 31 (2010) 192–203.
[18] E.M. Maria, et al., Comparison of different methods of spatial normalization of FDG-PET brain images in the voxel-wise analysis of MCI patients and controls, Ann. Nucl. Med. 27 (7) (2013) 600–609.
[19] N. Marwan, et al., Florbetapir PET, FDG PET, and MRI in Down syndrome individuals with and without Alzheimer's dementia, Alzheim. Dement. 11 (8) (2015) 994–1004.
[20] G. Mckhann, et al., Clinical diagnosis of Alzheimer's disease report of the NINCDS-ADRDA work group* under the auspices of department of health and human services task force on Alzheimer's disease, Neurology 34 (1984) 939–939.
[21] J.C. Morris, The Clinical Dementia Rating (CDR): current version and scoring rules, Neurology 43 (11) (1993) 2412–2414.
[22] L. Mosconi, Brain glucose metabolism in the early and specific diagnosis of Alzheimer's disease, Eur. J. Nucl. Med. Mol. Imag. 32 (4) (2005) 486–510.
[23] F. Nobili, et al., Unawareness of memory deficit in amnestic MCI: FDG-PET findings, J. Alzheimer's Dis. 22 (3) (2010) 993–1003.
[24] J. Platt, Sequential Minimal Optimization: A Fast Algorithm for Training Support Vector Machines, 1998, pp. 1–21. Technical Report MSR-TR-98-14.
[25] J.C. Rajapakse, et al., Statistical approach to segmentation of single-channel cerebral MR images, Med. Imag. IEEE Trans. 16 (1997) 176–186.
[26] R. Reitan, Validity of the trail making test as an indicator of organic brain damage, Percept Mot Ski 8 (1958) 271–276.

[27] L. Saint-Aubert, et al., Cortical florbetapir-PET amyloid load in prodromal Alzheimer's disease patients, EJNMMI Res. 3 (2013) 43.
[28] J.L. Shaffer, et al., Predicting cognitive decline in subjects at risk for Alzheimer disease by using combined cerebrospinal fluid, MR imaging, and PET biomarkers, Radiology 266 (2) (2013) 583–591.
[29] S.J. Son, et al., Connectivity analysis of normal and mild cognitive impairment patients based on FDG and PiB-PET images, Neurosci. Res. 98 (2015) 50–58.
[30] J. Stefan, et al., The relative importance of imaging markers for the prediction of Alzheimer's disease dementia in mild cognitive impairment—beyond classical regression, NeuroImage 8 (2015) 583–593.
[31] J. Sui, et al., Combination of resting state fMRI, DTI, and sMRI data to discriminate schizophrenia by N-way MCCA + jICA, Human Neurosci. 7 (2013) 235.
[32] H.I. Suk, et al., Discriminative group sparse representation for mild cognitive impairment classification, Mach. Learn. Med. Imag. Lect. Notes Comput. Sci. 8184 (2013) 131–138.
[33] H.I. Suk, et al., Hierarchical feature representation and multimodal fusion with deep learning for AD/MCI diagnosis, Neuroimage 101 (2014) 569–582.
[34] H.I. Suk, et al., Latent feature representation with stacked auto-encoder for AD/MCI diagnosis, Brain Struct. Funct. 220 (2) (2015) 841–859.
[35] C.L. Sutphen, et al., Longitudinal cerebrospinal fluid biomarker changes in preclinical Alzheimer disease during middle age, JAMA Neurol. 72 (9) (2015) 1029–1042.
[36] D.R. Thal, et al., [18F] flutemetamol amyloid positron emission tomography in preclinical and symptomatic Alzheimer's disease: specific detection of advanced phases of amyloid-β pathology, Alzheim. Dement. 11 (8) (2015) 975–985.
[37] J. Tohka, et al., Fast and robust parameter estimation for statistical partial volume models in brain MRI, Neuroimage 23 (2004) 84–97.
[38] N. Tzourio-Mazoyer, et al., Automated anatomical labeling of activations in SPM using a macroscopic anatomical parcellation of the MNI MRI single-subject brain, Neuroimage 15 (2002) 273–289.
[39] K.B. Walhovd, et al., Combining MR imaging, positron-emission tomography, and CSF biomarkers in the diagnosis and prognosis of Alzheimer disease, Am. J. Neuroradiol. 31 (2) (2010) 347–354.
[40] K.B. Walhovd, et al., Multi-modal imaging predicts memory performance in normal aging and cognitive decline, Neurobiol. Ag. 31 (7) (2010) 1107–1121.
[41] C.Y. Wee, et al., Enriched white matter connectivity networks for accurate identification of MCI patients, Neuroimage 54 (2011) 1812–1822.
[42] C.Y. Wee, et al., Identification of MCI individuals using structural and functional connectivity networks, Neuroimage 59 (3) (2012) 2045–2056.
[43] E. Westman, et al., Combining MRI and CSF measures for classification of Alzheimer's disease and prediction of mild cognitive impairment conversion, Neuroimage 62 (2012) 229–238.
[44] L. Xu, et al., Multi-modality sparse representation-based classification for Alzheimer's disease and mild cognitive impairment, Comput. Methods. Programs. Biomed. 122 (2) (2015) 182–190.
[45] L. Xu, et al., Prediction of progressive mild cognitive impairment by multi–modal neuroimaging biomarkers, J. Alzheim. Dis. 51 (4) (2016) 1045–1056.
[46] M. Yang, et al., Metaface learning for sparse representation based face recognition, in: Image Processing (ICIP), 2010 17th IEEE International Conference on, 2010, pp. 1601–1604.
[47] M. Yang, et al., Sparse representation based fisher discrimination dictionary learning for image classification, Int. J. Comput. Vis. 109 (3) (2014) 209–232.
[48] L. Yuan, et al., Multi-source feature learning for joint analysis of incomplete multiple heterogeneous neuroimaging data, Neuroimage 61 (3) (2012) 622–632.
[49] Q. Zhang, B. Li, Discriminative K-SVD for dictionary learning in face recognition, in: 2010 IEEE Conference on Computer Vision and Pattern Recognition (CVPR), 2010, pp. 2691–2698.
[50] D. Zhang, et al., Multimodal classification of Alzheimer's disease and mild cognitive impairment, Neuroimage 55 (3) (2011) 856–867.
[51] S. Zhang, et al., C-PIB-PET for the early diagnosis of Alzheimer's disease dementia and other dementias in people with mild cognitive impairment(MCI), NCBI 23 (7) (2014) CD010386.
[52] L. Zhou, et al., Hierarchical anatomical brain networks for MCI prediction: revisiting volumetric measures, PLoS One 6 (2011) e21935.
[53] Q. Zhao, et al., Quantitative multimodal multiparametic imaging in Alzheimer's disease, Brain Inform. 3 (2016) 29–37.
[54] X. Zhu, et al., A novel matrix-similarity based loss function for joint regression and classification in AD diagnosis, Neuroimage 100 (2014) 91–105.
[55] X. Zhu, et al., A novel multi-relation regularization method for regression and classification in AD diagnosis, Proc. Med. Image Comput. Comput. Assist. Intervent. 17 (3) (2014) 401–408.
[56] H. Zou, T. Hatie, Regularization and variable selection via the elastic net, J. R. Stat. Soc. 67 (2) (2005) 301–320.